Numerical Analysis of Liquid Metal MHD Flow and Heat Transfer for Open-surface Li Divertor in FNSF

Sergey Smolentsev, Charles E. Kessel, Jeremy D. Lore, Rajesh Maingi, Ranjit Singh, Dennis L. Youchison

***Abstract*— Within the ongoing US-based program on the development of liquid metal plasma facing components, numerical simulations and analysis are performed to address feasibility of the open-surface Li divertor. In the previous scoping studies (Smolentsev, 2021 [1]), divertor heat removal capabilities were assessed using a simplified flow model for a slug-type velocity profile and constant flow thickness. Here, new analyses take into account forces acting on the flowing Li layer. Three reduced order mathematical models are applied under the conditions of the US Fusion Nuclear Science Facility (FNSF) to access magnetohydrodynamic (MHD) flow development effects, velocity distribution, and surface waves: (1) fully developed MHD flow, (2) quasi-two-dimensional developing MHD flow, and (3) multiphase MHD flow. The obtained results for MHD flows and the surface heat flux computed with the plasma code SOLPS-ITER are then used as an input data to compute the temperature distribution in the divertor by solving the convection-diffusion energy equation.**

***Index Terms*— Divertor, Fusion Nuclear Science Facility, heat transfer, MHD, liquid metal, open-surface flow**

I. Introduction

A domestic liquid metal (LM) plasma-facing component (PFC) program was initiated by Fusion Energy Sciences (FES), USA in the fall of 2019 [2] following a system study in [3].

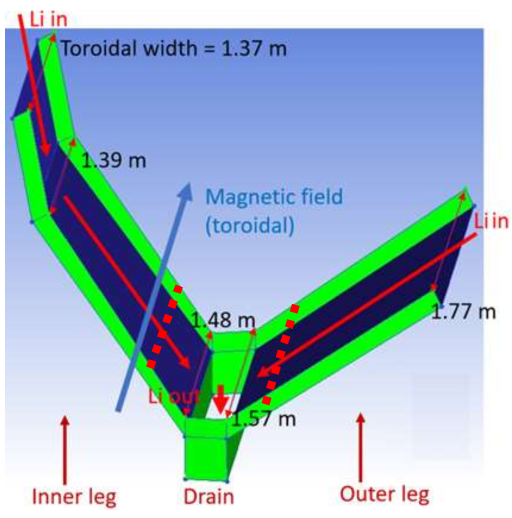

Fig. 1. Sketch of one 22.5° segment in the FNSF with the divertor cassette, including basic dimensions. The inner and outer legs and the drain at the bottom are shown. Locations of the two strike points are shown with the red dotted lines.

In this program, a generic flowing LM PFC is under consideration, where most of the high incident heat flux from plasma is removed by a thin open-surface lithium (Li) layer flowing down the helium-cooled (He) solid substrate of Reduced Activation Ferritic/Martensitic (RAFM) steel [1]. The ongoing design and analysis studies utilize the US Fusion Nuclear Science Facility (FNSF) [4] as a test-bed. A sketch of one 22.5° segment of the 16 toroidal segments in the FNSF with the divertor cassette is shown in Fig. 1. In this pre-conceptual design, "cold" liquid Li at 350°C enters the inner and outer divertor legs at the top and flows downwards absorbing high heat flux from plasma. The "hot" Li leaves the divertor at the bottom through the drain slot towards the ancillary equipment. In addition to Li, pressurized He gas flowing beneath or impinged [5] on the 5 mm RAFM substrate is used as a second coolant. The surface heat flux distributions computed with the SOLPS-ITER code [6] is shown in Fig. 2.

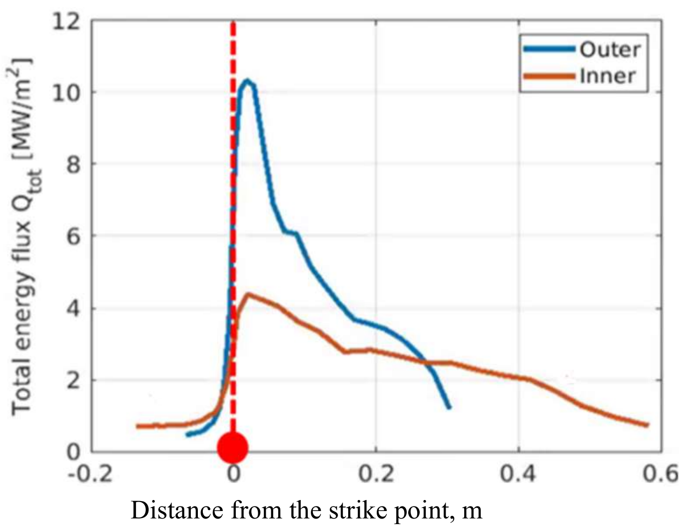

Fig. 2. Surface heat flux computed with the SOLPS-ITER code. Red circle shows location of the strike point.

Previous heat transfer analyses in [1] and [7] suggest three heat removal regimes: convection-dominated, diffusion-dominated and convection-diffusion. Of them, the convection-dominated regime was shown to provide the highest heat removal rate,

Manuscript received December xx, 2021; revised March xx, 2022. This work was supported by the U.S. Department of Energy under grants DE-SC0020979 and DEAC05-00OR22725 (*Corresponding author: S. Smolentsev*).

At the beginning of this study, S. Smolentsev was with the University of California, Los Angeles, USA and is now with the Oak Ridge National Laboratory, Oak Ridge TN, USA (e-mail: smolentsevsy@ornl.gov) . R. Singh is with the University of California, Los Angeles, USA.

C.E. Kessel, J.D. Lore and D.L. Youchison are with the Oak Ridge National Laboratory, Oak Ridge TN, USA.

R. Maingi is with the Princeton Plasma Physics Laboratory, Princeton NJ, USA.

Color versions of one or more of the figures in this article are available online at http://ieeexplore.ieee.org

such that a localized surface heat flux with the maximum at 10 MW/m^2 can be removed by a thin Li layer flowing at the velocity of the order of 10 m/s, while the maximum Li temperature at the Li free surface is kept below the evaporation limit of 450°C. As also shown, the He gas almost does not improve the overall heat removal rate but its use is still recommended as a safety measure to mitigate the risk of a substrate burn up in the unwanted event of Li dryout [8].

The main conclusions in [1] and [7] on the divertor heat transfer were drown, however, assuming a slug-type velocity profile and a constant thickness of the flowing Li layer. These simplifications are mitigated in the present study, where three MHD flow models are adopted to access the MHD flow effects and evaluate their influence on Li heat transfer.

II. Mathematical Models and Computer Codes

In general, depending on the balance of forces acting on the LM layer, the flow can demonstrate different regimes with respect to the variations of the flow thickness h with the axial distance x as sketched in Fig. 3. Such regimes were observed in the experiments on LM MHD flows in inclined chutes [9-12] and analyzed in computational and analytical studies [9-20]. For the given liquid metal choice, the parameters that can affect the flow are: the inlet velocity and nozzle height, magnetic field strength, inclination angle and toroidal width, flow length, and material of the substrate and lateral walls. Ideally, the selected parameters should guarantee the flow thickness in the divertor to be as uniform as possible as shown in Fig. 3a. In theory, a uniform flow can be achieved by adjusting the flow thickness at the inlet h_{in} close to the fully developed flow thickness h_{fd}. In practice, h_{fd} is often not known and even does not exist. One example is a hydraulic jump (Fig. 3d), where the flow reaches the critical thickness h_c undergoing an abrupt rise in the liquid surface. From the design standpoint such a regime is unacceptable.

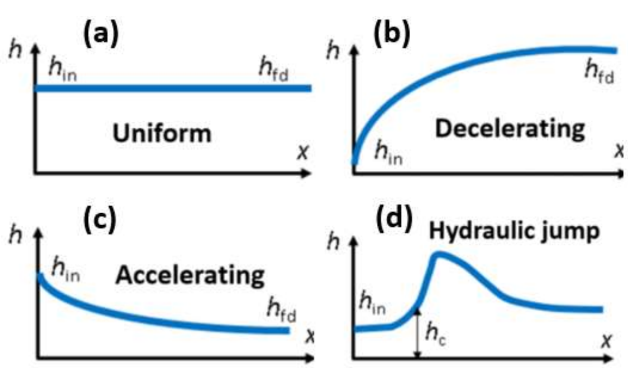

Fig. 3. Regimes of the open-surface LM MHD flow in an inclined chute in a magnetic field: (a) Uniform flow, h_{in}=h_{fd}; (b) Decelerating flow, h_{in}<h_{fd}; (c) Accelerating flow, h_{in}>h_{fd}; (d) Hydraulic jump, h_{in}<h_c<h_{fd}.

The specific features of the open-surface Li flow in the divertor cassette shown in Fig. 1 under the FNSF conditions are: high inlet velocity U_{in}~ 10 m/s as needed to remove high surface heat flux, relatively small thickness of the Li layer h_{in}~5-10 mm to reduce the Li inventory, steep inclination angle, large toroidal width of the chute $2b$ of about 1.5 m, and a short divertor length ~ 1 m. The flow occurs in a strong toroidal magnetic field B_{tor}~4-6 T. It can also be affected by a relatively small wall-normal magnetic field B_n~0.5 T. The associated Reynolds number $Re = \frac{U_{in}h_{in}}{\nu} \sim (0.5-1.2)\text{x}10^5$, Hartmann numbers $Ha_{tor} = B_{tor} b\sqrt{\frac{\sigma}{\nu\rho}} \sim (1.5-2.3)\text{x}10^5$ and $Ha_n = B_n \frac{h_{in}}{2}\sqrt{\frac{\sigma}{\nu\rho}} \sim$ ~(1.2-2.6)x10^2, Froude number $Fr = \frac{U_{in}^2}{gh_{in}}$~(1.0-2.0)x$10^3$, and the aspect ratio $\beta = \frac{h_{in}}{2b}$~(3.3-6.7)x$10^{-3}$. The Prandtl number of Li $Pr = \frac{\nu\rho C_p}{k}$ =0.035. Here, ρ, ν, σ, C_p, and k are the density, kinematic viscosity, electrical conductivity, specific heat, and thermal conductivity correspondingly. In this study, the properties of Li are taken as: ρ=485 kg/m^3, ν =8.5x10^{-7} m^2/s, σ =1.1x10^6 S/m, C_p=4200 J/kg K, and k=49.6 W/m K. In these range of the parameters, full 3D numerical computations of free surface MHD flows are very challenging and, to our best knowledge, no results have been reported in the literature. The mathematical models used in this study are of reduced order. They take into account the most important flow features associated with the influence of the applied magnetic field and the presence of the free surface but neglect those that appear to be less important. Concrete limitations of the utilized mathematical models are elaborated in the subsequent sections.

In all computations, special care was taken of the computational mesh. At least 10 points were placed within the Hartmann layers at the walls perpendicular to the magnetic field and about 15 points in the side layer at the substrate and within the boundary layer near the free surface.

A. Fully Developed MHD Flow

In a fully developed (fully established) flow, the flow thickness, the velocity and the induced magnetic field do not change with the axial coordinate x. The problem is governed by the 2D momentum equation for the axial velocity component $U(y,z)$ coupled with the 2D induction equation for the axial component of the induced magnetic field $B_x(y,z)$ [16]:

$$\nu\left(\frac{\partial^2 U}{\partial z^2} + \frac{\partial^2 U}{\partial y^2}\right) - \frac{1}{\rho}\frac{dP}{dx} + \frac{B_z^0}{\rho\mu_0}\frac{\partial B_x}{\partial z} = 0, \quad (1)$$

$$\frac{\partial}{\partial z}\left(\frac{1}{\sigma}\frac{\partial B_x}{\partial z}\right) + \frac{\partial}{\partial y}\left(\frac{1}{\sigma}\frac{\partial B_x}{\partial y}\right) + \mu_0 B_{tor}\frac{\partial U}{\partial z} = 0. \quad (2)$$

Here, μ_0 is the magnetic permeability of vacuum and $\frac{dP}{dx}$ is the pressure gradient in the fluid. The two elliptic PDEs are solved iteratively in the two-material domain that consists of the liquid metal and the solid electrically conducting lateral walls and substrate, using the Alternative Direction Implicit (ADI) method on a fine mesh that clusters the mesh point in the Hartmann layers at the lateral walls of the flow carrying chute, in the side layer at the bottom substrate, and in the special MHD boundary layer near the free surface. In this study, the computations are performed using a finite-difference code first developed in [16] and then modified for higher performance in [21].

B. Developing Q2D MHD Flow

The Q2D (quasi-two-dimensional) flow equations are obtained from the full 3D equations by their integration (averaging) in the direction of the applied magnetic field (z direction) between the two lateral walls, assuming a Hartmann-type velocity distribution in z. The lateral walls in the model are treated as either electrically conducting or insulating, depending on the wall conductance ratio $c_w = \frac{\sigma_w t_w}{\sigma b}$, which is zero in the case of the insulating walls. In the parameter range relevant to the divertor design, the electrical conductivity of the substrate is expected to have only a small effect on the MHD flow as the induced electric currents close their circuit inside the liquid through the side boundary layer at the substrate whose electrical resistance is much smaller than the electrical resistance of the RAFM substrate. That is why no effort has been made to incorporate the effect of the conducting substrate in the model. As a result of the integration, the problem is reduced to 2D in the (x,y) plane. In the new equations, the effect of the flow opposing electromagnetic Lorentz force is included through a special term on the RHS of the momentum equation. Such Q2D flow equations, also known as the SM82 model, were originally proposed in [22] for a non-conducting duct. An effort to extend this model to the case of electrically conducting duct was made in [23] under the name of "averaged flow model". A variant of the averaged model for open-surface MHD flows in a chute with either insulating or conducting lateral walls was developed in [13]. This model is based on the boundary layer (shallow water) approximation. The model and a computer code were further elaborated in [14], [20] and [24] to include heat transfer, flow effects due to the substrate curvature, and a non-uniform magnetic field. In this study, the developing MHD flows are computed using the most recent version of the numerical code as described in [20]. The governing equations are written here in the dimensionless form, using symbol "tilde" to indicate dimensionless quantities:

$$\frac{\partial \tilde{U}}{\partial \tilde{t}} + \tilde{U}\frac{\partial \tilde{U}}{\partial \tilde{x}} + \tilde{V}\frac{\partial \tilde{U}}{\partial \tilde{y}} = \frac{1}{Fr}\left(\sin(\alpha) - \frac{\partial \tilde{h}}{\partial \tilde{x}}\cos(\alpha)\right) - \beta^2\left(\frac{Ha_{tor}}{Re} + \frac{c_w}{1+c_w}\frac{Ha_{tor}^2}{Re}\right)\tilde{U}, \quad (3)$$

$$\frac{\partial \tilde{U}}{\partial \tilde{x}} + \frac{\partial \tilde{V}}{\partial \tilde{y}} = 0, \quad (4)$$

$$\frac{\partial \tilde{h}}{\partial \tilde{t}} + \tilde{U}_h\frac{\partial \tilde{h}}{\partial \tilde{x}} = \tilde{V}_h. \quad (5)$$

In this model, Eq. (3) is used to compute the velocity component U. Continuity equation Eq. (4) is used in the computations of the V component. Equation (5), the so-called kinematic free surface condition, serves for tracking the free surface by using computed velocities U_h and V_h at the free surface.

C. Multiphase MHD Flow Model in OpenFOAM

This model incorporates the MHD effects due to the applied toroidal magnetic field in the same way as in the Q2D MHD flow model, through a special electromagnetic term on the RHS of the momentum equation. Compared to the Q2D model, the new one includes several additional features, such as the full 2D momentum equation with the diffusion term retained, the volume of fluid (VOF) method for tracking liquid-gas interface, and surface tension forces. These new features were introduced through a user-defined model, using the MultiphaseEulerFoam module, a versatile solver in the open-source library OpenFOAM that computes the flow of multiple phases [25]. The main goal of using this model is to access possible surface wave formation and to evaluate the effect of surface tension. The model has successfully been tested against the recent computations with the Q2D model and earlier results in [14]. Some comparisons for the inner and outer divertor legs are shown in Fig. 7.

D. Heat Transfer

The heat transfer model is based on the unsteady 2D diffusion-convection energy equation for a multi-material domain of Li and solid substrate beneath the Li layer:

$$\rho C_p\left(\frac{\partial T}{\partial t} + U\frac{\partial T}{\partial x} + V\frac{\partial T}{\partial y}\right) = \frac{\partial}{\partial x}\left(k\frac{\partial T}{\partial x}\right) + \frac{\partial}{\partial y}\left(k\frac{\partial T}{\partial y}\right). \quad (6)$$

The boundary conditions are the prescribed surface heat flux, continuous temperature and heat flux at the interface between the RAFM substrate and Li , and convective cooling at the interface between substrate and the cooling He gas. The developed finite-difference code solves the energy equation in the computational domain of liquid and solid substrate in the (x,y) plane using the velocity components U and V computed with a fluid solver as the input data.

III. Results and Discussion

MHD flow and heat transfer results in this section are obtained for the divertor geometry and the surface heat flux shown in Fig.1 and 2. The length L and the inclination angle of the divertor plate α are L=0.72 m and α =73∘ for the inner leg, and L=0.36 m and α=43∘ for the outer leg. The Li flow thickness at the inlet h_{in} or the flow thickness h in the computations of the fully developed flow is 5 mm. The inlet velocity U_{in} is 6.5 m/s for the inner and 15.0 m/s for the outer divertor. These parameters are consistent with the previous heat transfer analysis in [1] to assure the maximum Li temperature at the free surface < 450∘C. The applied toroidal magnetic field is 5 T. The associated dimensionless parameters are: Ha_{tor}=1.94x10^5, Re=3.82x10^4 (inner divertor) and Re=8.82x10^4 (outer divertor). The aspect ratio is β=3.33x10^{-3}. The wall-normal magnetic field, which is roughly 10 times lower than the toroidal magnetic field, is not taken into account. As shown in [20], its effect on the flow is important for a toroidally continuous divertor, but small in the case of a segmented divertor. The dividing lateral walls in the analysis are assumed to be electrically non-conducting to reduce high MHD drag and associated rise of the flow thickness.

In the heat transfer computations, the boundary condition at the substrate takes into account He cooling with high heat transfer coefficient of 20 000 W/m^{2}K. However, in the convection-dominated regime, the He flow has only a small or no effect on the temperature field in the Li layer. Therefore, it is not discussed in this paper. Detailed analysis of the He flow effects in different heat removal regimes can be found in [1]. The Li inlet temperature in all computations is 350◦C.

A. Fully Developed Flow and Heat Transfer

For the inlet flow thickness significantly different from the flow thickness of its fully developed flow, the simulations for a developing flow suggest the flow development length in excess of 10 m, whereas the divertor length is shorter than 1 m. Nevertheless, the analysis of a fully developed flow is important for characterization of the MHD velocity profile and its effect on heat transfer. The computed velocity profile in a fully developed flow is shown in Fig. 4.

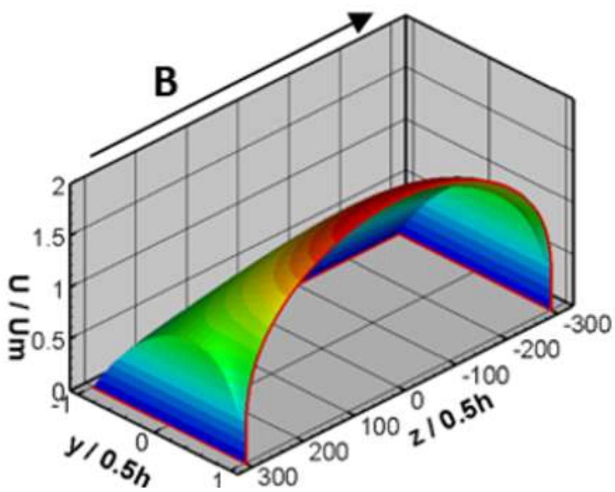

Fig. 4. Computed velocity profile in the fully developed flow.

The distinctive feature of the flow is a significantly higher velocity at the free surface compared to the mean velocity. Such a velocity pattern is favorable for heat removal as seen in Fig. 5, where the comparisons are made for the Li temperature at the free surface between the MHD flow and the slug flow.

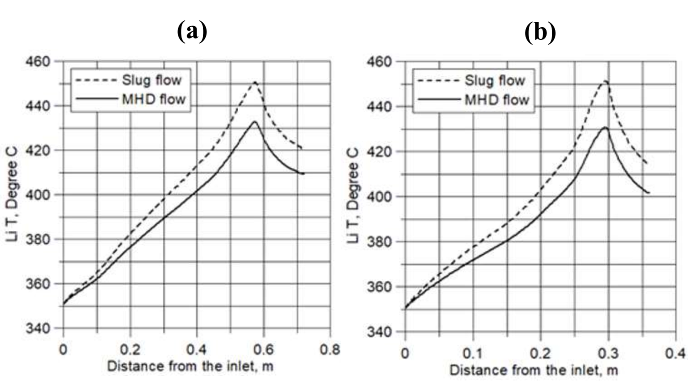

Fig. 5. Li surface temperature: (a) in the inner, and (b) outer divertor. The mean velocity U_m is 6.5 m/s (inner) and 15 m/s (outer divertor).

The MHD flow allows for about 20K lower temperature at the strike point compared to the slug flow. This is a substantial reduction of ~ 20% with respect to the maximum temperature rise. Further heat transfer analysis that uses the MHD velocity profile and limits the max Li temperature at the free surface at 450◦C, suggests that the mean velocity could be reduced compared to the slug flow from 15 m/s to 10 m/s for the outer leg, and from 6.5 m/s to 4.5 m/s for the inner leg.

B. Q2D Developing Flow and Heat Transfer

Computational results are shown in Fig. 6 for the Li flow thickness as a function of the axial coordinate and for the temperature distribution at the free surface for both the inner and the outer divertor. The downstream variations of the Li layer thickness in Fig. 6a and b for three magnetic fields 4, 5 and 6 T show that the flow in the inner divertor is accelerating, while that in the outer divertor is decelerating.

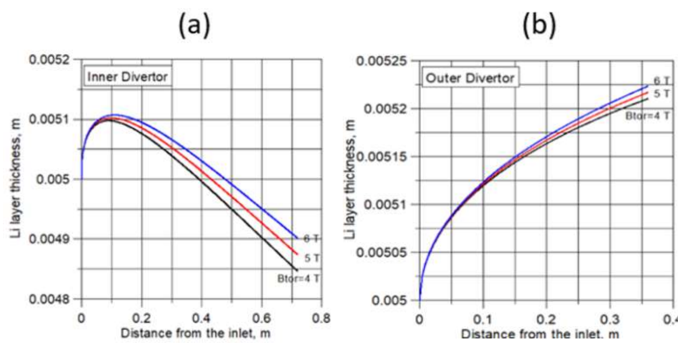

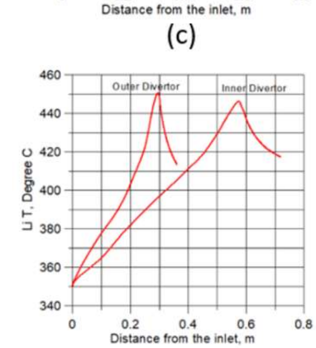

Fig. 6. Computed thickness of the Li layer and surface temperature, using the Q2D developing flow model. (a) Flow thickness variations, inner divertor, and (b) outer divertor. (c) Li surface temperature at B_{tor}=5 T.

The difference is obviously related to the steeper inclination angle of the inner divertor and different velocities. However, due to the high velocity and a relatively short divertor length, in both cases, the relative changes of the flow thickness are insignificant, smaller than 5%. Also, the differences in the flow thickness related to the magnitude of the applied toroidal magnetic field are small, not exceeding 1%. As a matter of fact, the flow is in the early development stage, such that the slug flow can serve as a reasonable approximation. It is not surprising that the results of the heat transfer computations in Fig. 6c are very close to those in Fig. 5 for the slug flow.

C. Multiphase Flow

The use of VOF in OpenFOAM implies a second phase, a gas, in addition to liquid Li. In the present computations, argon (Ar) gas is used. The flows were computed without surface tension (σ_t=0) first, and then with the surface tension (σ_t=0.53 N/m). Comparisons are shown in Fig. 7 for the time-averaged flow thickness. The figure also shows the flow computed with the Q2D code. All three computations are close, suggesting that the effects of the surface tension force and viscous friction at the Li free surface on the time-averaged flow are small.

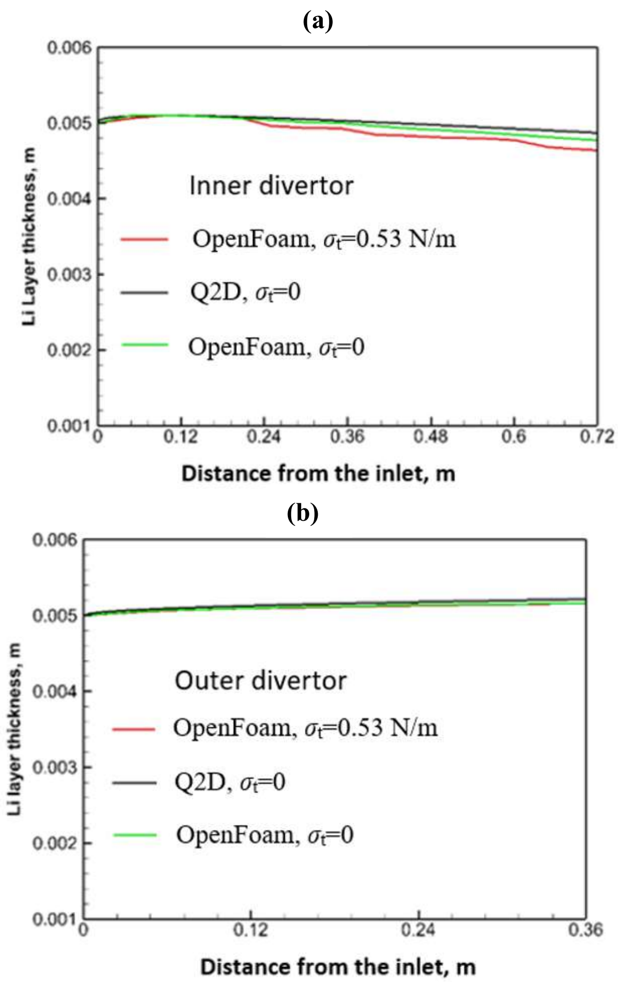

Fig. 7. Thickness of the Li layer computed with OpenFOAM and using the Q2D flow model: (a) Inner divertor, and (b) Outer divertor. OpenFOAM results are time averaged.

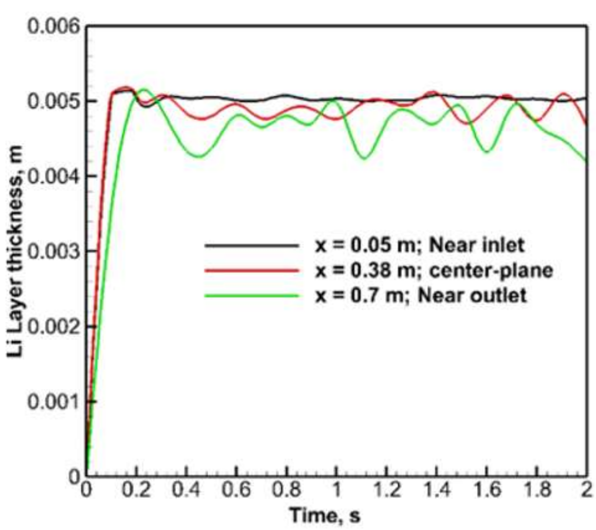

Fig. 8. Time-dependent Li flow thickness at three axial locations computed with OpenFOAM with surface tension included.

An instantaneous flow is illustrated in Figs. 8 and 9 for the inner divertor. Unlike the time-averaged flow, the effect of surface tension is significant. Including surface tension in the computations results in a lesser disturbed interface. However, even in the presence of surface tension forces, the interface is wavy as seen in Fig. 9.

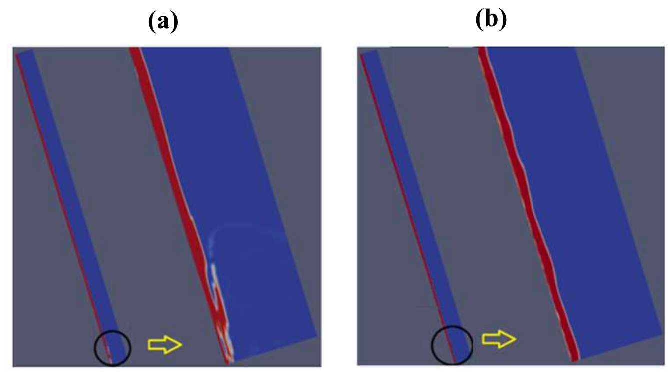

Fig. 9. Surface waves at the Li / gas interface. Inner divertor. (a) Li flow computed without surface tension, and (b) with surface tension at 0.1 s. Red and blue color indicate Li and Ar.

The disturbances appear first at the inlet and move downstream with the main flow, growing in time. As seen in Fig. 8, the wave amplitude increases with the axial distance reaching about 10% of the time-averaged flow thickness at the outlet. The flow remains unbroken over the entire flow path as the divertor is short and the velocity is high.

IV. Conclusion

Various flow features were addressed in the computations for the open-surface Li divertor for the US Fusion Nuclear Science Facility, using three reduced order flow models. The fully developed flow model suggests that the MHD velocity profile is more favorable for removal of high surface heat flux from plasma compared to the slug flow that was used in the previous heat transfer analysis. As shown, such a velocity profile can allow for reduction of the mean velocity by a factor of 1.5 due to higher velocity at the free surface. The Q2D MHD flow model has demonstrated some flow development effects: accelerating flow in the inner and decelerating in the outer divertor. However, due to the high flow velocity and the short divertor length resulting in strong inertia effects, the changes in the flow thickness are smaller than 5%, suggesting that the flow in the divertor is in the early development stage. The multiphase flow model indicates that the Li flow in the divertor can be unstable due to development of surface waves. These waves, however, do not cause flow disintegration as the maximum wave amplitude at the divertor exit does not exceed 10% of the mean flow thickness. Present heat transfer computations are in general consistent with the previous heat transfer results obtained under the assumption of a slug-type flow. All these observations suggest that a near-uniform, high velocity open-surface Li flow that meets heat transfer requirements of a low vaporization divertor can be established. However, this conclusion has to be further supported through physical experiments and full 3D computations.

REFERENCES

[1] S. Smolentsev, "Design window for open-surface lithium divertor with helium-cooled substrate," *Fusion Eng. Des*., vol. 173, p. 112930, 2021.

[2] D. Andruczyk, R. Maingi, C. Kessel, D. Curreli, E. Kolemen *et al*., "A domestic program for liquid metal PFC research in fusion," *J. Fusion Energy*, vol. 39(6), pp. 441-447, 2020.

[3] C.E. Kessel, D. Andruczyk, J.P. Blanchard, T. Bohm, A. Davis *et al*., "Critical exploration of liquid metal plasma-facing components in a Fusion Nuclear Science Facility," *Fusion Sci. Technol*., vol. 75, pp. 886-917, 2019.

[4] C. E. Kessel, J. P. Blanchard, A. Davis, L. El-Guebaly, N. Ghoniem *et al*., "The Fusion Nuclear Science Facility, the critical step in the pathway to fusion energy," *Fusion Sci. Technol*., vol. 68, pp. 225-236, 2015.

[5] M.S. Tillack, R. Raffray, R. Wang, S. Malang, S. Abdel-Khalik, M. Yoda, D. Youchison, "Recent US activities on advanced He-cooled W-alloy divertor concepts for fusion power plants," *Fusion Eng. Des*., vol. 86 , pp. 71–98, 2011.

[6] J.D. Lore, C. Kessel, D. Curreli, R. Maingi, M. Rezazadeh, S. Smolentsev, "Simulation of liquid lithium divertor geometry using SOLPS-ITER." 19th IEEE Symposium on Fusion Engineering (SOFE-2021), December 13-16, 2021.

[7] S. Smolentsev, T. Rhodes, Y. Jiang, P. Huang, C. Kessel, "Status and progress of liquid metal thermofluids modelling for the US Fusion Nuclear Science Facility," *Fusion Sci. Technol*., DOI: 10.1080/15361055.2021.1906134, 2021.

[8] M. Szott, D.N. Ruzic, "2-D moving mesh modeling of lithium dryout in open surface liquid metal flow applications," *Fusion Eng. Des*., vol. 154, p. 111512, 2020.

[9] T.N. Aitov, A.B. Ivanov, A.V. Tananaev, "Flow of liquid metal in a chute in a coplanar magnetic field," *Magnetohydrodynamics*, vol. 23, pp. 78-82, 1987.

[10] V.V. Baranov, I.A. Evtushenko, I.R. Kirillov, E.V. Firsova, V.V. Yakovlev, "Liquid metal flow for fusion application," *Magnetohydrodynamics*, vol. 30, pp. 460-467, 1994.

[11] M. Narula, A. Ying, M.A. Abdou, "A study of liquid metal film flow under fusion relevant magnetic fields," *Fusion Sci. Tech*., vol. 47, pp. 562–569, 2005.

[12] A. Shishko, F. Muktepavela, A. Klukin, E. Platacis, A. Sobolev, "The effect of the divertor poloidal magnetic field on liquid metal thin film flow," *Magnetohydrodynamics*, vol. 50, pp. 207-216, 2014.

[13] T.N. Aitov, E.M. Kirillina, "Flow of electrically conducting liquid in a thin layer with free surface under the action of a strong magnetic field," *Magnetohydrodynamics*, vol. 21, pp. 71-76, 1985.

[14] I.A. Evtushenko, S.Yu. Smolentsev, A.V. Tananaev, "Hydrodynamics and exchange of heat in thin liquid-metal layers within a magnetic field," *Magnetohydrodynamics*, vol. 27, pp. 287-290, 1991.

[15] A.Ya. Shishko, "A theoretical investigation of steady-state film flows in a coplanar magnetic field," *Magnetohydrodynamics*, vol. 28, pp. 170-181, 1992.

[16] V.M. Kudrin, S.Yu. Smolentsev, A.V. Tananaev, "Developed flow of a thin liquid metal layer in an inclined magnetic field," *Magnetohydrodynamics*, vol. 29, pp. 66-70, 1993.

[17] L. Chungpin, M.S. Kazimi, B. LaBombard, "MHD effects on liquid metal film flow," *Nucl. Eng. Des*., vol. 146, pp. 325-335, 1994.

[18] H. Huang, A. Ying, M. Abdou, "3D MHD free surface fluid flow simulation based on magnetic-field induction equations," *Fusion Eng. Des*., vol. 63–64, pp. 361-368, 2002.

[19] S. Siriano, A. Tassone, G. Caruso, "Numerical simulation of thin-film MHD flow for nonuniform conductivity walls," *Fusion Sci. Tech*., vol. 77, pp. 144-158, 2021.

[20] S. Smolentsev, T. Rognlien, M. Tillack, L. Waganer, C. Kessel, "Integrated liquid metal flowing first wall and open-surface divertor for Fusion Nuclear Science Facility: concept, design, and analysis," *Fusion Sci. Technol*., vol. 75, pp. 939-958, 2019.

[21] S. Smolentsev, N. Morley, M. Abdou, "Code development for analysis of MHD pressure drop reduction in a liquid metal blanket using insulation technique based on a fully developed flow model," *Fusion Eng. Des*., vol.73, pp. 83-93, 2005.

[22] J. Sommeria, R. Moreau, "Why, how, and when, MHD turbulence becomes two-dimensional," *J. Fluid. Mech*., vol. 118, pp. 507–518, 1982.

[23] S.Yu. Smolentsev, "Averaged model in MHD duct flow calculations," *Magnetohydrodynamics*, vol. 33, pp. 42-47, 1997.

[24] S. Smolentsev, M. Abdou, "Open-surface MHD flow over a curved wall in the 3-D thin-shear-layer approximation," *Appl. Math. Model*., vol. 29, pp. 215-234, 2005.

[25] The OpenFOAM Foundation Ltd. OpenFOAM version 9. https://openfoam.org/version/9/.

Sergey Smolentsev obtained his Ph.D. in Thermophysics from the Leningrad Polytechnic University, Russia in 1990 and performed his postdoctoral study on instabilities in liquid metal flows at Ben Gurion University of Negev, Israel under supervision of Prof. Herman Branover. From 1990 he worked as a Professor at the St. Petersburg Polytechnic University, and in 1998 joined the University of California, Los Angeles (UCLA). Since 2022, he is a distinguished staff member at Oak Ridge National Lab, US.

He served as task leader/coordinator/developer in various US national and international projects on fusion blankets and Liquid Metal (LM) plasma-facing components, such as the Advanced Power Extraction Study (APEX, 1998-2003), ITER Test Blanket Module (2003-2012), US-JAPAN JUPITER/TITAN Collaboration on Liquid Breeders (2001-2012), US-INDIA Collaboration on LM MHD/Heat Transfer for PbLi blankets (2015-2017) and Fusion Engineering System Studies/Fusion Nuclear Science Facility in the US (2015-2019). As project leader in a collaboration with EUROfusion on blanket development (2015-2019), he was responsible for the design and construction of the one-of-a-kind Magnetohydrodynamic PbLi Experiment (MaPLE) at UCLA. His research accomplishments in the area of fusion blanket design and analysis, liquid metal MHD and heat & mass transfer have been published in about 150 scientific articles.